AUTOPHAGY
2023, VOL. 19, NO. 11, 2869–2883
https://doi.org/10.1080/15548627.2023.2233847

Taylor & Francis
Taylor & Francis Group

RESEARCH PAPER

Foot-and-mouth disease virus structural protein VP3 interacts with HDAC8 and promotes its autophagic degradation to facilitate viral replication

Huijun Zhang[a,b], Xiangwei Wang[a], Min Qu[a], Zhiyong Li[c], Xiangping Yin[a], Lijie Tang[b], Xiangtao Liu[a], and Yuefeng Sun[a]

[a]State Key Laboratory for Animal Disease Control and Prevention, College of Veterinary Medicine, Lanzhou University, Lanzhou Veterinary Research Institute, Chinese Academy of Agricultural Sciences, Lanzhou, China; [b]Department of Preventive Veterinary Medicine, College of Veterinary Medicine, Northeast Agricultural University, Harbin, Heilongjiang, China; [c]School of Basic Medical Sciences, Wenzhou Medical University, Wenzhou, Zhejiang, China

ABSTRACT

Macroautophagy/autophagy has been utilized by many viruses, including foot-and-mouth disease virus (FMDV), to facilitate replication, while the underlying mechanism of the interplay between autophagy and innate immune responses is still elusive. This study showed that HDAC8 (histone deacetylase 8) inhibits FMDV replication by regulating innate immune signal transduction and antiviral response. To counteract the HDAC8 effect, FMDV utilizes autophagy to promote HDAC8 degradation. Further data showed that FMDV structural protein VP3 promotes autophagy during virus infection and interacts with and degrades HDAC8 in an AKT-MTOR-ATG5-dependent autophagy pathway. Our data demonstrated that FMDV evolved a strategy to counteract host antiviral activity by autophagic degradation of a protein that regulates innate immune response during virus infection.

Abbreviations: 3-MA: 3-methyladenine; ATG: autophagy related; Baf-A1: bafilomycin A_1; CCL5: C-C motif chemokine ligand 5; Co-IP: co-immunoprecipitation; CQ: chloroquine phosphate; DAPI: 4″,6-diamidino-2-phenylindole; FMDV: foot-and-mouth disease virus; HDAC8: histone deacetylase 8; ISG: IFN-stimulated gene; IRF3: interferon regulatory factor 3; MAP1LC3/LC3: microtubule associated protein 1 light chain 3; MOI: multiplicity of infection; MAVS: mitochondria antiviral signaling protein; OAS: 2″–5′-oligoadenylate synthetase; RB1: RB transcriptional corepressor 1; SAHA: suberoylanilide hydroxamic acid; TBK1: TANK binding kinase 1; $TCID_{50}$: 50% tissue culture infectious doses; TNF/TNF-α: tumor necrosis factor; TSA: trichostatin A; UTR: untranslated region.

ARTICLE HISTORY
Received 27 October 2022
Revised 16 June 2023
Accepted 3 July 2023

KEYWORDS
Autophagy; FMDV; histone deacetylase 8; virus replication; innate immune response

Introduction

Autophagy is a major degradative pathway for eliminating cytosolic materials during normal development and adverse conditions [1–4]. Autophagy is a process that comprises induction, nucleation, expansion, fusion, and degradation. More than 40 genes regulating this process have been identified in yeast, fungi, and mammals, emphasizing the conservation of this pathway [5]. MTOR (mechanistic target of rapamycin kinase), a highly conserved kinase, initiates autophagy under adverse conditions, such as hunger, oxidative stress, energy deprivation, and pathogen infection [6,7]. The inhibition of MTOR activates a protein complex composed of ULK1/ULK2, RB1CC1, ATG13 and ATG101, which leads to autophagosome formation [5]. Additionally, PIK3C3/VPS34 and PIK3R4/VPS15, along with BECN1, mediate the nucleation step [8]. The phosphatidylinositol-3-phosphate (PtdIns3P) gathered at the membrane nucleation site needs to recruit more ATG proteins to start phagophore expansion and membrane closure [8]. In contrast, ATG7 and ATG10 act to generate the ATG12–ATG5 conjugate, which, along with ATG16L1, ATG7 and ATG3 function in lipidation of Atg8-family proteins, regulating steps including autophagosome fusion with the lysosome and degradation of subcellular constituents [1,5,8–10]. Autophagy regulates various cellular processes, including viral infection, which interferes with the life cycle of viruses by opposing viral entry, inhibiting virus replication through the degradation of viral components, and modulating the antiviral response [11–14]. In response, viruses also evolved strategies to resist, escape, or counteract the autophagic process [5].

Foot-and-mouth disease virus (FMDV), a single-stranded positive-sense RNA virus, is the causative agent of foot-and-mouth disease (FMD), a highly contagious viral disease of cloven-hoofed animals, belongs to the type species of the *Aphthovirus* genus within the *Picornaviridae* family [15]. FMDV genome consists of a 5' untranslated region (UTR), an integral open reading frame/ORF, and a 3'UTR with a poly (A) tail. The open reading frame encodes a polyprotein, which is subsequently cleaved into at least 14 proteins, such as leader proteinase (Lpro), VP1, VP2, VP3, VP4, 2A, 2B, 2C, 3A, 3B1, 3B2, 3B3, $3C^{pro}$, and $3D^{pol}$ [15,16]. Many studies have shown that FMDV can manipulate autophagy to facilitate virus replication. FMDV non-structural proteins 2B, 2C, and 3A colocalize with the autophagosome marker LC3, and more importantly, chemical stimulation or inhibition of the autophagy process correlated with an increase or decrease of virus

CONTACT Yuefeng Sun sunyuefeng@caas.cn State Key Laboratory for Animal Disease Control and Prevention, College of Veterinary Medicine, Lanzhou University, Lanzhou Veterinary Research Institute, Chinese Academy of Agricultural Sciences, Lanzhou 730000, China
Supplemental data for this article can be accessed online at https://doi.org/10.1080/15548627.2023.2233847

production [17]. In another report, FMDV 2C can interact with BECN1 to prevent the fusion of autophagosomes with lysosomes, allowing for virus survival [18]. Berryman *et al.* also showed that FMDV can induce autophagosomes during cell entry to facilitate infection via a class III phosphatidylinositol 3-kinase-independent pathway [19]. FMDV capsid protein VP2 can induce autophagy through the EIF2S1-ATF4-AKT-MTOR cascade; further investigation showed that VP2 induces autophagy via interaction with HSPB1 protein [20]. FMDV 3A interacts with G3BP1 and promotes its autophagic degradation by upregulating the expression of autophagy-related protein LRRC25, eventually inhibiting IFN signaling and host innate antiviral response [21]. Also, researchers showed that FMDV replication depends on the expression of EIF2AK3/PERK and the autophagy marker LC3B-II, as inhibiting the EIF2AK3/PERK pathway and autophagy significantly restricted virus replication [22]. A recent study showed that FMDV-induced ER stress response and autophagy depend on STING1, as knockdown/knockout of STING1 suppresses FMDV replication and viral protein expression [23]. Although the involvement of autophagy in the positive regulation of FMDV replication has been reported, some controversial studies also showed that FMDV-induced autophagy does not promote viral replication or even suppress FMDV replication [24,25]. Researchers showed that FMDV induces the activation of PERK and ATF6-mediated UPR but does not influence the replication of FMDV [26]. More interestingly, Fan *et al.* demonstrated that FMDV suppresses autophagy and viral protein production, and ATG12-ATG5 positively regulates antiviral NFKB/NF-κB and IRF3 signaling during FMDV infection, thereby limiting FMDV proliferation [27]. A recent study by Wu *et al.* showed that SEC62 interacts with LC3 to attenuate ER stress and FMDV replication by recruiting and delivering autophagosomes into the lysosome for clearance [28]. The above findings demonstrated the importance of autophagy involved in the regulation of FMDV replication, but the underlying mechanism of autophagy during FMDV infection is far from understood and needs further investigation.

Histone deacetylases (HDACs, also named lysine deacetylases, KDACs), together with histone acetylases (HAT, also named lysine acetylases, KATs), were originally found to regulate gene expression by altering the structure of chromatin [29–32]. Nevertheless, more and more researchers found that HDACs participate in many cellular processes by deacetylating non-histone proteins [33–36], such as tissue development, cell cycle, neuronal diseases, cancer formation, and virus replication [37–42]. To date, 18 human HDACs have been recognized that are grouped into four classes based on their sequence homology to yeast HDACs, class I (HDAC1-HDAC3, and HDAC8), class II (HDAC4-HDAC7, HDAC9, and HDAC10), class III (SIRT1 through SIRT7), class IV (HDAC11) [35,43]. HDAC8 belongs to class I, and several papers have reported its involvement in virus replication. After the vaccinia virus infection, HDAC8 was shown to translocate from nuclear to cytosol, which suggests the vaccinia virus can recruit nuclear proteins to replication complexes for use in viral processes [44]. Another study showed that HDAC1 and HDAC8 repress IFNB/IFN-β expression, while HDAC6 acts as a coactivator essential for enhancer activity [45]. Similarly, Meng *et al.* showed that Rb, a well-known tumor suppressor, protects mice from RNA and DNA virus infection by suppressing IFNB production through HDAC1 and HDAC8 [46]. In 2011, Yamauchi *et al.* showed that HDAC8 could efficiently promote productive entry of influenza A virus in tissue culture cells depletion of HDAC8 inhibited IAV infection but promoted VSV replication [47]. Contrary to the above reports, Xia *et al.* demonstrated that *MIR21-3p* could promote influenza A virus replication by targeting HDAC8 3'UTR and suppressing its expression [48]. The function of HDAC8 in virus replication is far from understood and needs further exploration.

In this study, we showed that FMDV infection promotes the degradation of HDAC8, and knockout of *HDAC8* in different cell lines significantly increases the replication of FMDV. Mechanism study demonstrated that HDAC8 participated in the regulation of antiviral response. To counteract this effect, FMDV structural protein VP3 interacts with and promotes HDAC8 autophagic degradation to facilitate virus replication, and further investigation found that HDAC8 degradation is mediated through AKT-MTOR pathway and knockout of *ATG5* blocked VP3 induces HDAC8 degradation. Our data reported the interplay between innate immune response and autophagy during FMDV infection, which provides a therapeutic intervention candidate for future study.

Results

FMDV infection induced HDAC8 degradation in a time and dose-dependent manner

Previous reports have shown the involvement of HDAC8 in virus replication. Western-blot and Real-time PCR were performed to check HDAC8 expression and explore the change of HDAC8 during FMDV infection. As shown in Figure 1A–D, in PK-15 cells, with the increasing infection time and multiplicity of infection (MOI), HDAC8 protein expression level decreased gradually, while there was no obvious change of *HDAC8* mRNA; similar data were also obtained in BHK-21 cells, FMDV infection induced the decrease HDAC8 protein, not mRNA (Figure 1E–H). FMDV (VP0, VP3, VP1) polyclonal antibody was used to monitor viral replication by western blot. Viral titrations were also quantified to show viral replication, and the expression level of HDAC8 was normalized with TUBB/β-tubulin or GAPDH. From the above results, we speculated that HDAC8 might involve FMDV replication.

Inhibition or knockout of HDAC8 increased FMDV replication in BHK-21 and PK-15 cells

HDACs inhibitors are widely used to inhibit deacetylase activity. Among them, SAHA and TSA are universal inhibitors of HDAC1 to HDAC11, MGCD0103 is the inhibitor of HDACs class I, PCI34051 is an HDAC8 specific inhibitor, nicotinamide (NIC) is the inhibitor of SIRT1 to SIRT7 [49–52]. Different cell lines (BHK-21 and PK-15) were treated with these inhibitors after FMDV infection, and a western blot was performed to monitor viral replication. As shown in

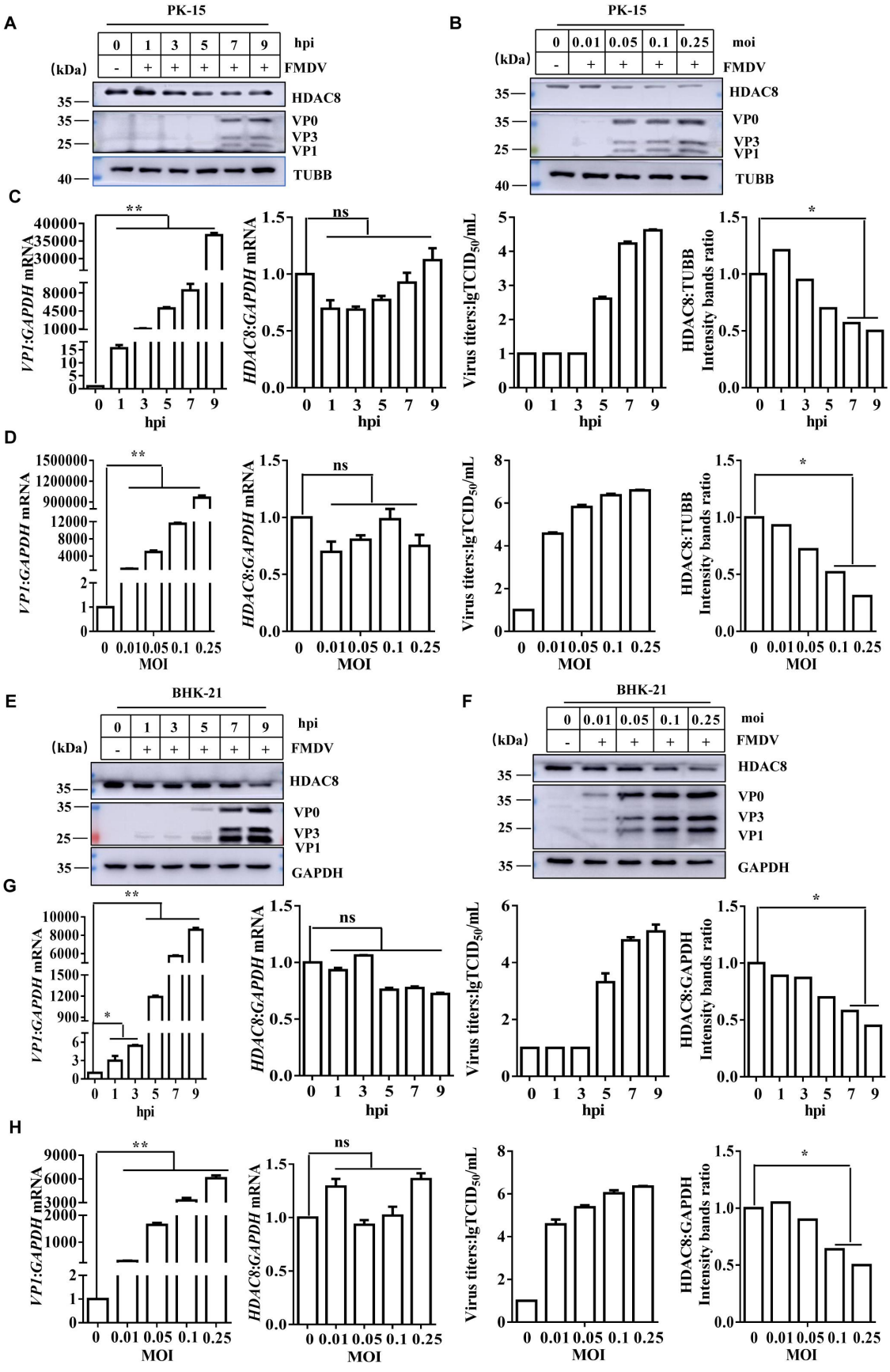

Figure 1. FMDV infection decreases HDAC8 protein but not mRNA expression level. (A, C) PK-15 cells were infected with FMDV (0.1MOI) for 0, 1, 3, 5, 7, or 9 h, and endogenous HDAC8 and viral VP0, VP3, and VP1 proteins were detected by western blot, and viral RNA and *HDAC8* mRNA were detected by qPCR. Viral titration and quantitative analysis of the HDAC8:TUBB densitometry ratio were estimated. (B, D) PK-15 cells were mock-infected or infected with 0.01, 0.05, 0.1, or 0.25 MOI of FMDV at 8 h. Endogenous HDAC8 and viral VP0, VP3, VP1 proteins were detected by western blot, and viral RNA and *HDAC8* mRNA were detected by qPCR. Viral titrations and quantitative analysis of the HDAC8:TUBB densitometry ratio were estimated. (E, G) BHK-21 cells were infected with FMDV (0.1MOI) for 0, 1, 3, 5, 7, or 9

Figure 2A,B, compared with control (DMSO treated) cells, treatment with SAHA, TSA, MGCD0103, and PCI34051 significantly increased virus replication (shown in FMDV polyclonal antibody expression), while treatment with NIC does not affect virus replication. These data demonstrated the involvement of HDAC8 in regulating FMDV replication.

To further confirm our results, CRISPR-Cas9 technique was employed to knock out the *HDAC8* gene in two cell lines (PK-15 and BHK-21 cell lines). As shown in Figure 2C, D, compared with control cells, the two *HDAC8* knockout cell lines showed no HDAC8 protein expression (In PK-15 and BHK-21 cells), which clearly shows the success of knockout of *HDAC8* protein expression. The genome sequencing results are also consistent with the western blot results. In PK-15 cells, clone 1 has one nucleotide insertion in the second exon, and clone 2 has two nucleotides insertion in the second exon (Fig. S1A, B, and C); while in BHK-21 cell lines, compared with wildtype *HDAC8* gene, the knockout clone 1 has two nucleotides insertion in the second exon, clone 2 has four nucleotides deletion in the second exon, this lead to the early termination of protein translation (Fig. S2A, B, and C). Then, the cell growth curve was created, and the results showed no significant difference in growth rate between *HDAC8*-KO cell lines and NC, suggesting that the *HDAC8*-KO cell lines could be extended indefinitely with a steady growth rate (Fig. S1D and S2D). Viral replication was quantified between control and knockout cells to test the effect of HDAC8 dysfunction. As shown in Figure 2C, FMDV replication was measured by Real-time PCR, western blot, and viral titration, all of the results demonstrated that virus replication was increased in *HDAC8* knockout cells compared with control cells. In BHK-21 cells, similar data was also obtained (Figure 2D). Altogether, these data demonstrated that HDAC8 could inhibit FMDV replication.

HDAC8 participates in the activation of innate immune responses

Innate immunity is the first line of defense against virus infection. To investigate the function of HDAC8 in the regulation of immune response, control and *HDAC8* knockout cell lines were used to detect the expression of interferon-related genes. As shown in Figure 3A, FMDV polyclonal antibody was used to detect the expression of FMDV structural proteins. Compared with control cells, in PK-15 cell line knockout of *HDAC8* significantly reduced the phosphorylation of TBK1 and IRF3 during FMDV infection, which are key regulators of interferon production and subsequent immune response, resulting in increased viral replication in knockout cells. In addition, overexpression of HDAC8 in PK-15 cell line significantly potentiated the phosphorylation of TBK1 and IRF3 during FMDV infection. Then it weakened the viral replication (Figure 3B). Also, Real-time PCR results showed that the expression level of IFNB, IFIT2/ISG54, CCL5, OAS, and TNF significantly decreased in *HDAC8* knockout cells and increased in HDAC8 overexpression cells compared with control cells (Figure 3C,D). These data consistently showed that HDAC8 regulates innate immune response during FMDV infection.

FMDV structural protein VP3 is responsible for the degradation of HDAC8

Since HDAC8 suppressed the replication of FMDV, our previous data showed that FMDV evolved to degrade HDAC8. Different FMDV gene plasmids were transfected into PK-15 cells to explore the underlying mechanism. Western-blot showed the expression of different FMDV proteins by anti-FLAG antibody (Figure 4A), compared with control (Empty vector transfection), transfection of VP2, VP3, and $3C^{pro}$ plasmids showed a decreased expression of HDAC8, others showed no obvious difference (Figure 4A). VP2 has been shown to activate the cellular EIF2S1-ATF4 pathway and induce autophagy via HSPB1, which may also lead to the degradation of HDAC8 [20]. 3Cpro is a known protease to universally cleave host proteins to facilitate FMDV replication [53,54], so we focused on VP3 protein for further study. As shown in Figure 4B,E, the expression of transfected or endogenous HDAC8 degraded dose-dependent with the transfection of O strain FMDV VP3 plasmid. FMDV had seven serotypes, serotype A and Asia I VP3 plasmids were constructed and co-transfected with HDAC8 into cells to test whether the VP3 protein of other serotypes could degrade HDAC8 expression. As shown in Figure 4C,D,F,G, these two VP3 proteins also induced HDAC8 degradation in a dose-dependent manner, suggesting that VP3-induced HDAC8 degradation is conserved through all three FMDV serotypes.

VP3 interacts with HDAC8 and promotes its autophagic degradation

Previous data showed that VP3 promotes HDAC8 degradation, so we speculated that VP3 might interact with HDAC8. As we expected, co-transfection of HA-HDAC8 and FLAG-VP3 plasmids into HEK293T cells, after immunoprecipitated with anti-HA antibody, we can detect VP3 with Anti-FLAG antibody (Figure 5A), after immunoprecipitated with anti-FLAG antibody, HDAC8 was detected by western-blot (Figure 5B). Further immunofluorescence data also show the colocalization of HDAC8 with VP3 (Figure 5C). To examine whether VP3 interacted with the HDAC8 during FMDV infection, the FMDV-infected cell lysates were immunoprecipitated with anti-HDAC8 antibody and probed for the presence of VP3. HDAC8 pulled down VP3 in

h, and endogenous HDAC8 and viral VP0, VP3, and VP1 proteins were detected by western blot, and viral RNA and *HDAC8* mRNA were detected by qPCR. Viral titrations and quantitative analysis of the HDAC8:GAPDH densitometry ratio were estimated. (F, H) BHK-21 cells were mock-infected or infected with 0.01, 0.05, 0.1, or 0.25 MOI of FMDV at 8 h. Endogenous HDAC8 and viral VP0, VP3, VP1 proteins were detected by western blot, and viral RNA and *HDAC8* mRNA were detected by qPCR. Viral titrations and quantitative analysis of the HDAC8:GAPDH densitometry ratio were estimated.

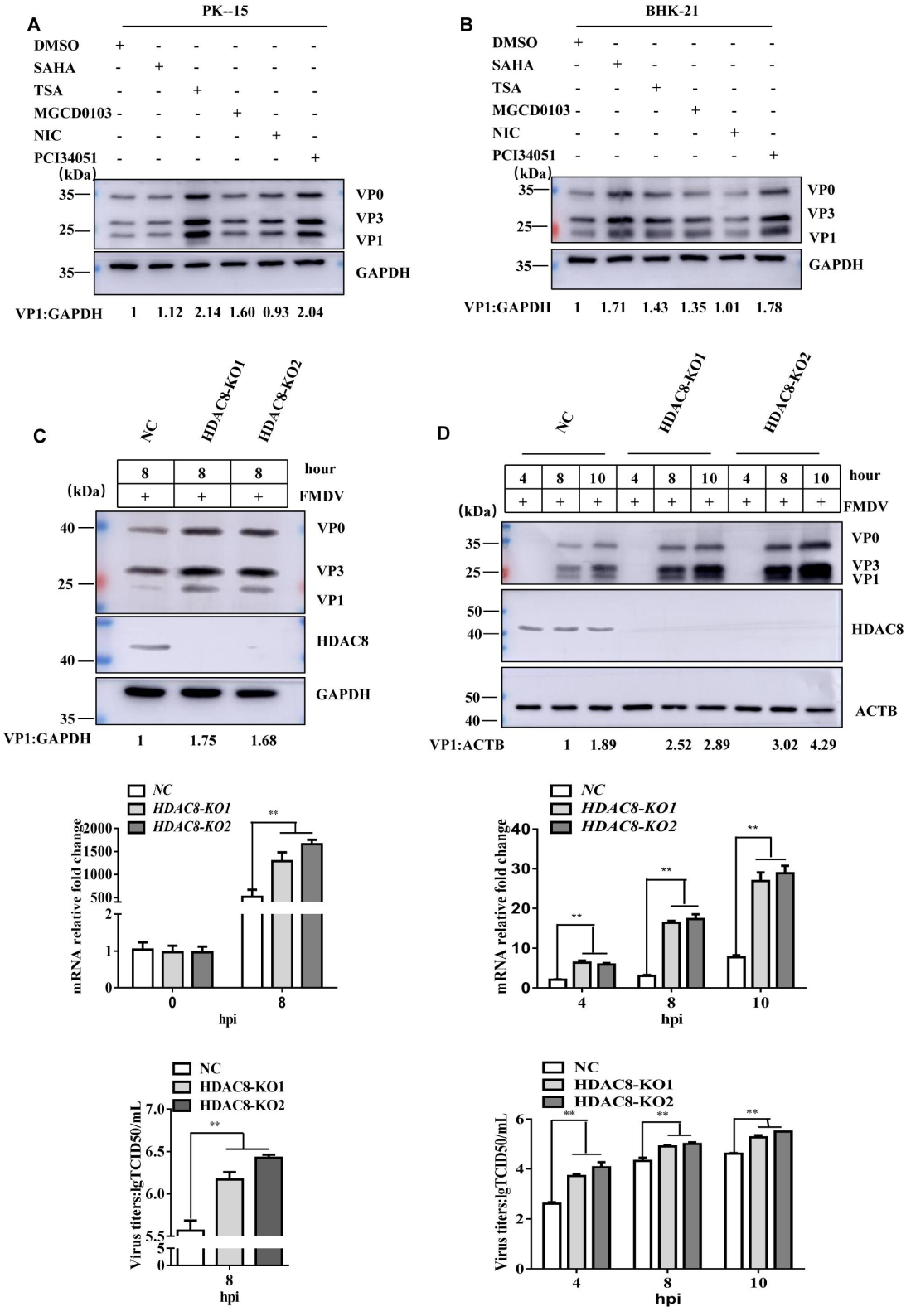

Figure 2. HDAC8 dysfunction promotes FMDV replication. (A, B) PK-15 cells and BHK-21 cells were seeded in 6-well plates to reach an approximate 90% confluence and infected with FMDV at an MOI of 0.1. The cells were incubated for 1 h and treated with HDAC inhibitors SAHA (10 μM), TSA (10 μM), MGCD0103 (10 μM), NIC (5 μM), or PCI34051 (5 μM). Samples were collected at 8 h post-infection, and viral protein was determined by western blot with indicated antibodies. (C) NC and *HDAC8*-KO PK-15 cells were infected with FMDV for 8 h, and the expression of viral proteins or mRNA and titers was detected by western blot, qPCR, and $TCID_{50}$ assay. (D) NC and *HDAC8*-KO BHK-21 cells were infected with FMDV for 4, 8, or 10 h, and the expression of viral proteins or mRNA and viral titration was detected by western blot, qPCR, and $TCID_{50}$ assay.

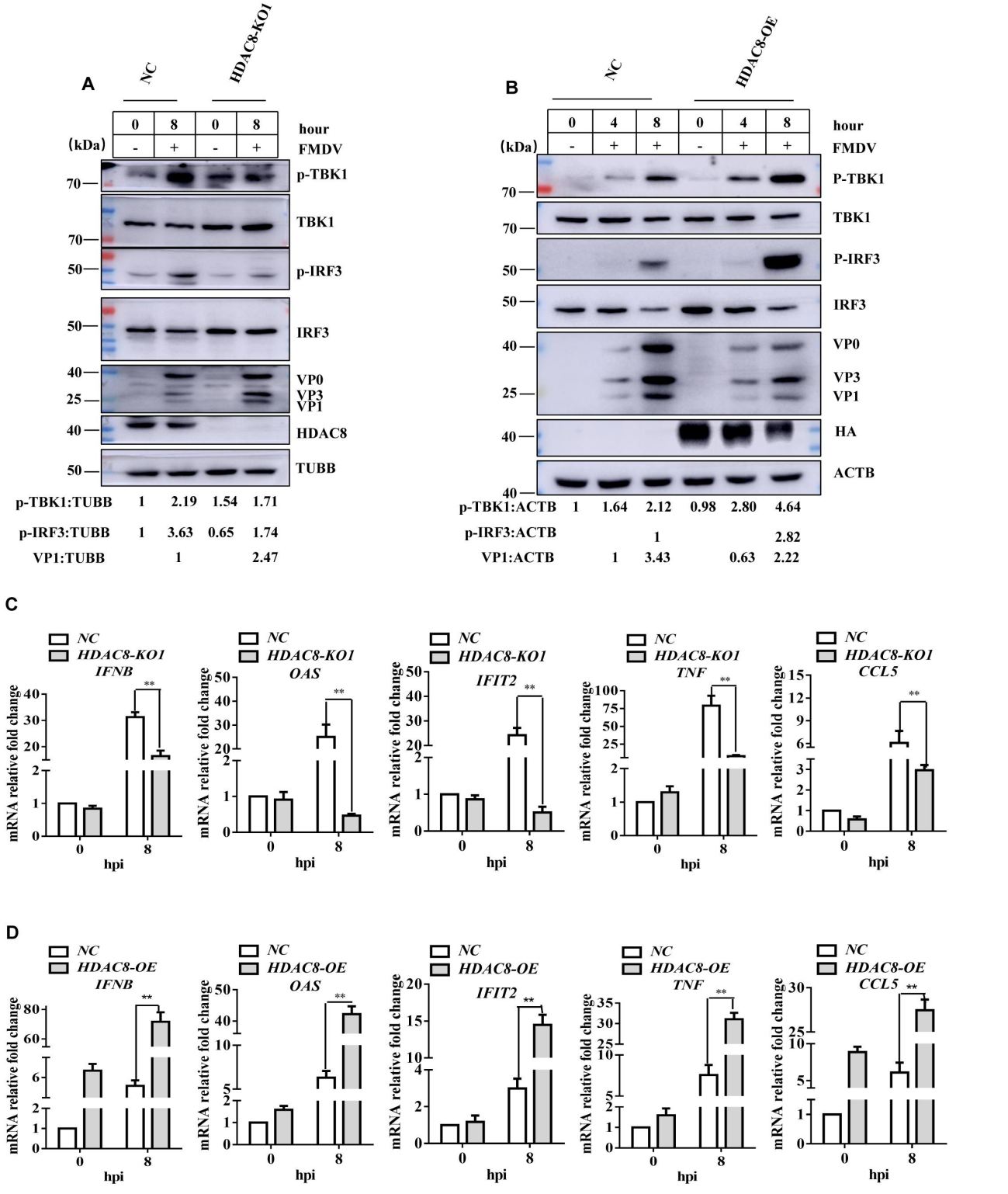

Figure 3. HDAC8 involves in the antiviral signaling pathway. (A) NC and *HDAC8*-KO1 PK-15 cells were seeded in 60-mm dishes and infected with FMDV at an MOI of 0.1, and samples were collected at 8 h post-infection. The p-TBK1, TBK1, p-IRF3, IRF3, VP0, VP3, VP1, HDAC8, and TUBB protein levels were detected by western blot. (B) PK-15 cells were transfected with 2 μg of HA-HDAC8 plasmid or empty vector for 24 h and then infected with FMDV (0.1 MOI) for 0, 4, or 8 h. The expression level of p-TBK1, TBK1, p-IRF3, IRF3, VP0, VP1, VP3, HDAC8, and ACTB proteins were detected by western blotting. (C) NC and *HDAC8*-KO1 PK-15 cells were seeded in 60-mm dishes and infected with FMDV at an MOI of 0.1, and samples were collected at 8 h. The *IFNB*, *OAS*, *IFIT2*, *TNF*, and *CCL5* mRNA levels were detected by qPCR. (D) PK-15 cells were transfected with 2 μg of HA-HDAC8 plasmid or empty vector for 24 h and then infected with FMDV (0.1 MOI) for 0 or 8 h. The *IFNB*, *OAS*, *IFIT2*, *TNF*, and *CCL5* mRNA levels were detected by qPCR. $^{**}p < 0.01$; $^{*}p < 0.05$.

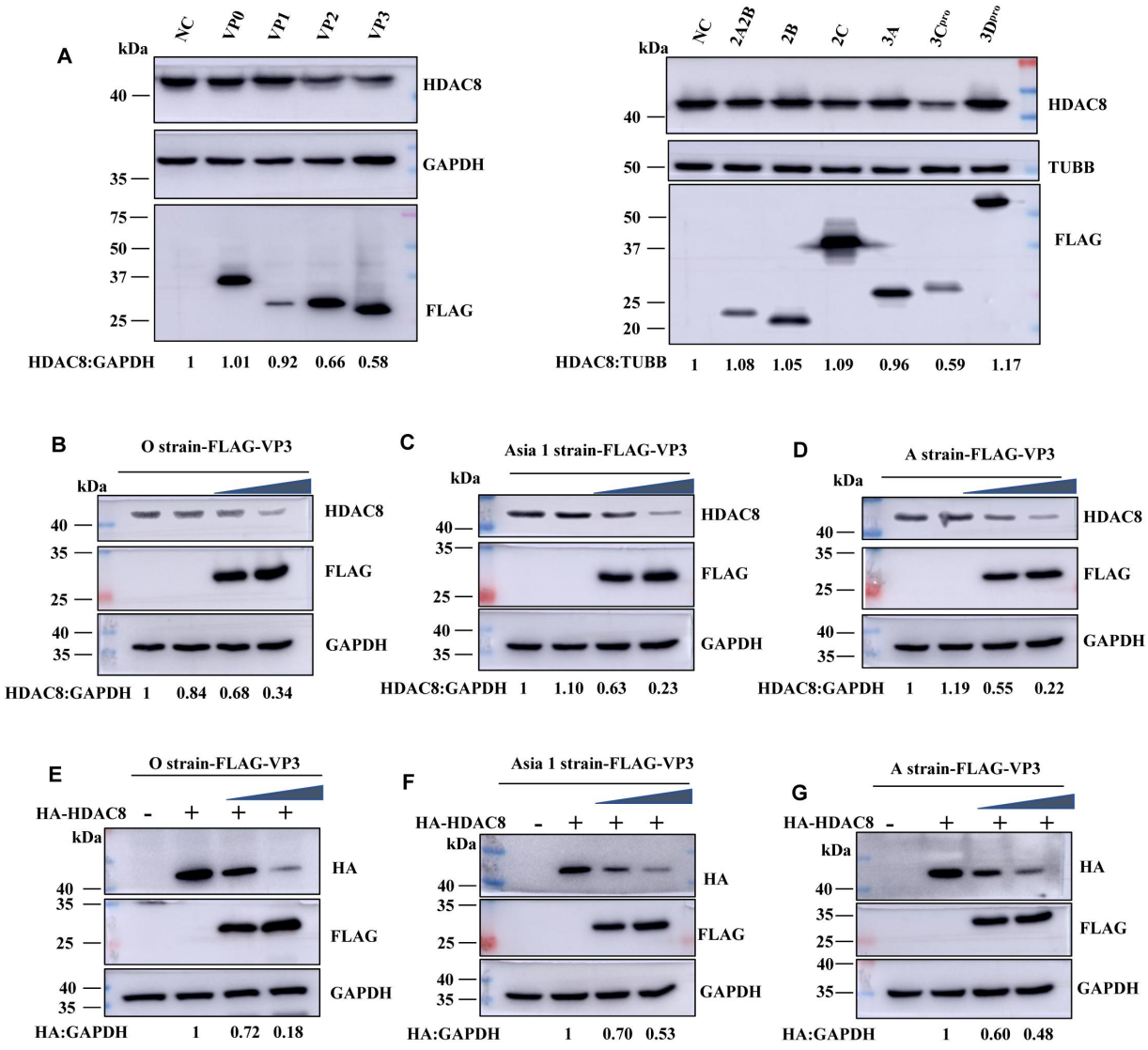

Figure 4. FMDV VP3 protein is responsible for reducing HDAC8 expression. (A) PK-15 cells were transfected with 2 μg plasmid expressing various FLAG-tagged viral proteins. At 24 h, endogenous HDAC8 protein was determined by western blot. (B, C, D) PK-15 cells were seeded in 6-well plates, and the monolayer cells were transfected with 0, 1.0, 2.0 μg FLAG-VP3 (O strain, Asia 1 strain, or A strain) plasmid for 24 h. Expression of endogenous HDAC8 was determined by western blot. (E, F, G) PK-15 cells were seeded in 6-well plates, and the monolayer cells were co-transfected with 0, 1.0, 2.0 μg FLAG-VP3 (O strain, Asia 1 strain or A strain) and 1.0 μg HA-HDAC8 plasmid for 24 h. Expression of HA-HDAC8 was determined by western blot.

FMDV-infected cells, and immunofluorescence data also show the colocalization of endogenous HDAC8 with FLAG-VP3 (Fig. S3A and S3D). These data consistently showed the interaction between HDAC8 and VP3. Different deletion mutations of VP3 plasmids were constructed and co-transfected with HDAC8 to clarify the specific region of VP3 interacting with HDAC8. Immunoprecipitation results showed that the N and C terminus of VP3 is not responsible for the interaction with HDAC8, only the VP3 (316–465) plasmid showed the interaction (Figure 5D,F). The immunofluorescence data also showed the colocalization of these two proteins (Fig. S4A). Next, to verify the region of VP3 responsible for the degradation of HDAC8, different deletions of VP3 plasmids were co-transfected with HDAC8 into PK-15 cells. Western-blot results showed that VP3 316–465 and VP3 466–660 could promote the degradation of HDAC8 (Figure 5E). The previous report has shown that cAMP signaling inhibited the degradation of HDAC8 via autophagy and the ubiquitin-proteasome system by reducing MAPK/JNK activity [55]. To verify which degradation pathway is involved during FMDV infection, different inhibitors of degradation pathways were added to the culturing cells co-transfected with VP3 and HDAC8. As shown in Figure 5G and Fig. S5, the addition of autophagy degradation pathway inhibitor 3-MA, CQ, and Baf-A_1 showed significant recovery of HDAC8 expression, while the addition of ubiquitin degradation pathway inhibitor MG132 does not show an obvious recovery of HDAC8 expression. As a control, we co-

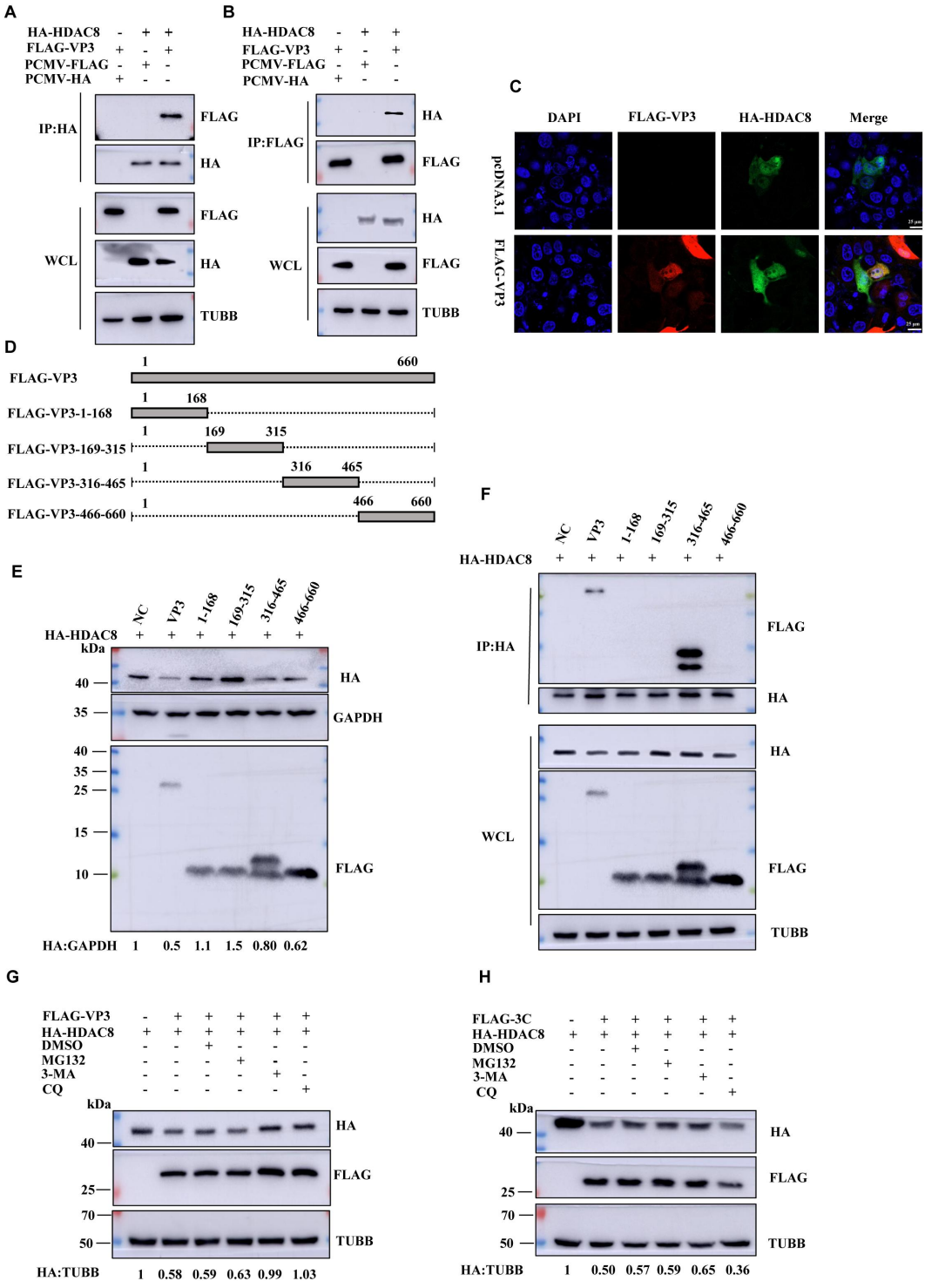

Figure 5. VP3 interacts with and degrades HDAC8 via the autophagy pathway. (A, B) HEK293T cells were transfected with the indicated plasmids, and cell lysates were immunoprecipitated with FLAG or HA antibodies, followed by a western blot with indicated antibodies. (C) PK-15 cells were co-transfected with FLAG-VP3 plasmids or empty vector and HA-HDAC8 plasmid for 24 h. Cells were incubated with anti-FLAG (red), anti-HA (green), and DAPI (blue) for immunofluorescence staining and analyzed by confocal microscopy. (D) Schematic representation showing a series of FLAG-tagged truncated VP3 mutants. (E) PK-15 cells were co-transfected with HA-HDAC8 and FLAG-VP3 plasmids or truncated FLAG-VP3 plasmids. The expression of these proteins was detected by western blot with indicated antibodies. (F) HEK293T cells were transfected with the indicated plasmids, and cell lysates were immunoprecipitated with a HA antibody, followed by a western blot with HA and FLAG antibodies. (G) PK-15 cells were co-transfected with FLAG-VP3 (O strain) and HA-HDAC8 plasmids and maintained in the presence or absence of MG132 (20 μM), 3-MA (10 mM), CQ (100 μM) for 24 h. The expression of HDAC8 and VP3 proteins were detected by western blot. (H) PK-15 cells were co-transfected with FLAG-3C and HA-HDAC8 plasmids and maintained in the presence or absence of MG132 (20 μM), 3-MA (10 mM), and CQ (100 μM) for 24 h. The expression of HDAC8 and 3C proteins were detected by western blot.

transfected FMDV 3C plasmid with HDAC8. The addition of inhibitors cannot restore the expression of HDAC8 (Figure 5H). These data demonstrated the function of FMDV VP3 protein in promoting the degradation of HDAC8 in an autophagic pathway.

VP3 promotes HDAC8 degradation through an AKT-MTOR-ATG5-dependent pathway

The conversion of soluble LC3 into membrane-bound LC3-phosphatidylethanolamine (PE) is an important event in autophagy. Membrane-bound LC3-PE controls several key processes in autophagy, including growth and expansion of the phagophore, recruitment of cargoes, and fusion of autophagosomes and lysosomes [4,56]. AKT plays a key part in the maintenance of the activity of MTOR through the AKT-MTOR pathway [57]. Western blot was performed to test the expression of LC3 to investigate if VP3 promotes autophagy. As shown in Figure 6A, compared with control, transfection of VP3 in PK-15 cells inhibited the phosphorylation of AKT and MTOR, thus leading to the increased expression of LC3B-II. Consistent with western blot data, the expression of VP3 increased the accumulation of fluorescent puncta of LC3B (Figure 6B), which clearly showed the induction of autophagy. Electron microscopy is one of the most commonly used methods to detect autophagy. As shown in Figure 6C, compared with the control, there were more vesicles after VP3 transfection, which had typical characteristics of autophagic vesicles. Next, the interaction of VP3 with LC3 was explored. More interestingly, we found the interaction of VP3 with LC3 by reciprocal co-immunoprecipitation and immunofluorescence experiments (Figure 6D–F). To examine whether VP3 interacted with LC3 during FMDV infection, the FMDV-infected cell lysates were immunoprecipitated with anti-LC3B antibody and probed for the presence of VP3. LC3 pulled down VP3 in FMDV-infected cells, and immunofluorescence data also show the colocalization of endogenous LC3 with FLAG-VP3 (Fig. S3B and S3E). These results implied the function of VP3 in the regulation of autophagy. Besides LC3, levels of SQSTM1/p62 also can be used to monitor autophagic. SQSTM1 is selectively incorporated into autophagosomes through direct binding to LC3 and is efficiently degraded by autophagy, and thus the total cellular expression levels of SQSTM1 inversely correlate with autophagic activity [58]. Compared with the control, the protein level of SQSTM1 is significantly reduced with the transfection of VP3 (Figure 6A). And then, the interaction of VP3 with SQSTM1 was detected by reciprocal immunoprecipitation experiments (Figure 6G,H). Furthermore, the immunofluorescence data also show the colocalization of VP3 and SQSTM1 (Figure 6I). To examine whether VP3 interacted with SQSTM1 during FMDV infection, the FMDV-infected cell lysates were immunoprecipitated with anti-SQSTM1/p62 antibody and probed for the presence of VP3. SQSTM1 pulled down VP3 in FMDV-infected cells, and immunofluorescence data also show the colocalization of endogenous SQSTM1 with FLAG-VP3 (Fig. S3C and S3F). FLAG-VP3 and HA-HDAC8 plasmids were co-transfected into PK-15 cells to investigate the pathway involved in the autophagic degradation of HDAC8. As shown in Figure 6J, VP3-induced LC3 puncta were colocalized with HDAC8, which demonstrated the degradation of HDAC8. SC79 (a specific AKT activator) was used to activate the AKT in the cytoplasm, inhibit AKT membrane translocation, and then promote the phosphorylation of AKT. As shown in Figure 6K, compared with control cells, VP3 could degrade the expression of HDAC8, but with the treatment of SC79, the expression of HDAC8 was recovered in a dose-dependent manner. Also, the phosphorylation of AKT and MTOR recovered with the increasing dose treatment of SC79. *ATG5* is a well-known gene regulating autophagy, a PK-15-*ATG5* knockout cell line was used to investigate whether ATG5 participates in HDAC8 degradation. Co-transfection of VP3 and HDAC8 plasmids in PK-15-*ATG5* knockout cells could no longer induce the degradation of HDAC8 (Figure 6L), and more interestingly, compared with control, knockout of *ATG5* reduced FMDV replication in PK-15 cells (Fig. S6). The above data demonstrated that VP3 induced HDAC8 autophagic degradation in AKT-MTOR-ATG5-dependent pathway.

Discussion

Autophagy has long been recognized to regulate virus replication. Several studies have found that FMDV utilized autophagy to facilitate its replication, but the detailed mechanism needs to be discovered. This study found that HDAC8, a histone deacetylase regulating antiviral response and the expression of immune response genes, was degraded by FMDV structural protein VP3 in an AKT-MTOR-ATG5-dependent autophagic pathway (Figure 7). The following experiments verified these above results. Firstly, FMDV infection promoted the degradation of HDAC8, and knockout of *HDAC8* facilitated the replication of FMDV, which demonstrated the regulation function of HDAC8 in FMDV replication; Secondly, transfection of VP3 inhibited the phosphorylation of AKT and MTOR, promoted HDAC8 degradation, while a specific AKT activator SC79 or deletion of *ATG5* recovered the expression of HDAC8 with the co-transfection of VP3, this implied the autophagic degradation of HDAC8 was mediated by FMDV VP3 protein; Thirdly, VP3 not only interacted with HDAC8 but also with LC3 and SQSTM1 to promote autophagy, the colocalization of HDAC8 with LC3 in the cytosol after VP3 transfection was verified by immunofluorescence experiments. Our data built the connection between autophagy and immune response during FMDV infection.

Upon viral nucleic acid sensing, pattern-recognition receptors, such as TLRs, RLRs, and other sensors, activate signaling pathways for the host's defense, including NF-KB and IFN pathways [59,60]. Through this, interferon provides the first line of defense against invading viruses. Accumulating evidence demonstrated that autophagy regulates host immunity [61]. Porcine circoviruses type 2 (PCV2) could promote the K48-linked ubiquitination of CGAS and subsequent autophagic degradation to facilitate virus replication [62]. Furthermore, influenza A virus subtype H7N9 PB1 protein was shown to recruit host E3 ligase RNF5 to MAVS and lead to its autophagic degradation [63]. SARS-CoV-2 helicase NSP13 can promote the autophagic degradation of TBK1, the central kinase in the IFN pathway, in cooperation with

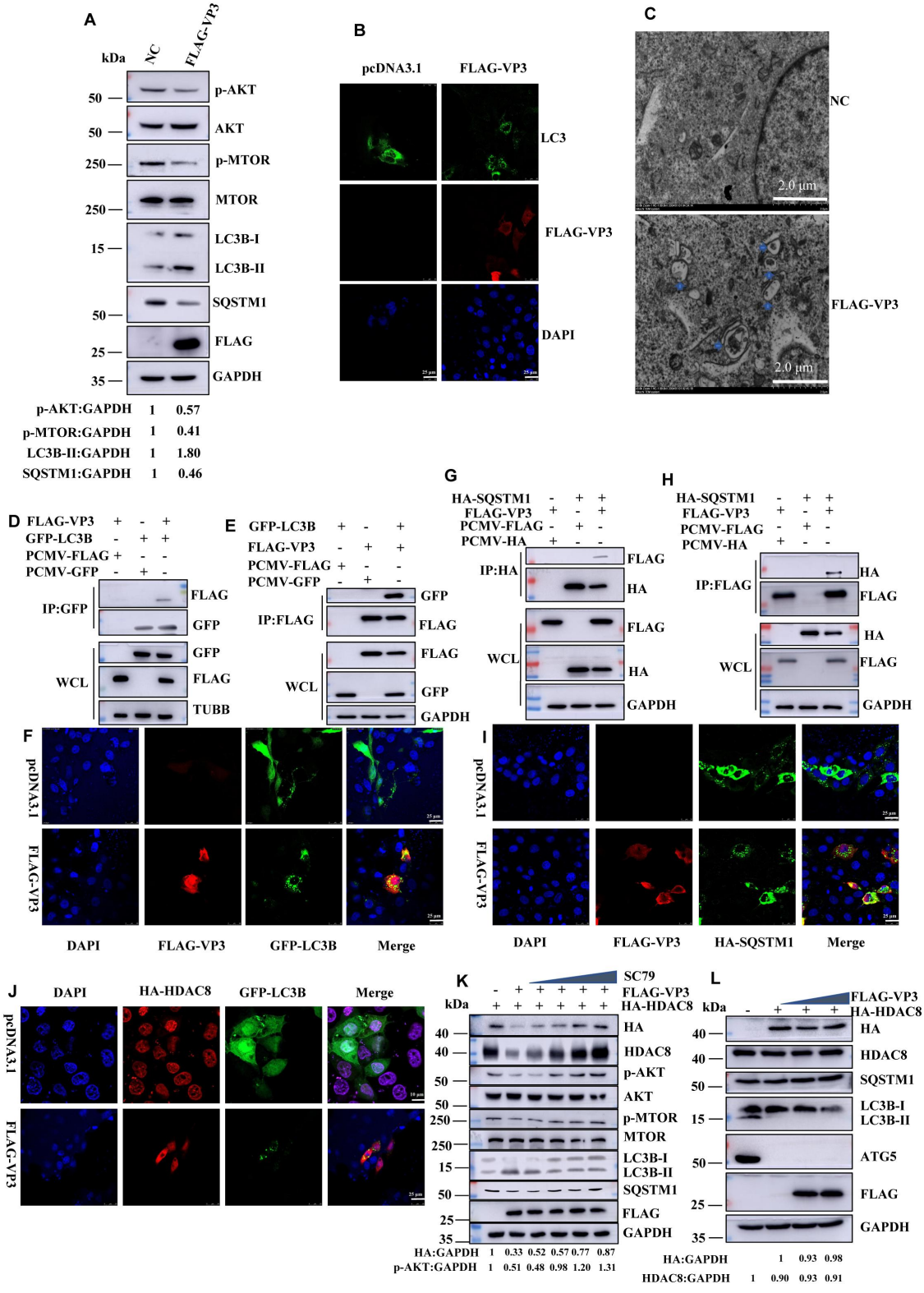

Figure 6. VP3 induces autophagy and degrades HDAC8 via the AKT-MTOR-ATG5-dependent pathway. (A) PK-15 cells were transfected with empty vectors or FLAG-VP3 for 24 h. LC3B, SQSTM1, AKT, p-AKT, MTOR, p-MTOR, and FLAG were analyzed by western blot. GAPDH was used as a control to show the even loading of samples. (B) PK-15 cells were transfected with FLAG-VP3 or empty vectors for 24 h, cells were fixed and analyzed by immunofluorescence using anti-LC3B antibodies, and the fluorescence signals were visualized by confocal microscopy. (C) PK-15 cells were transfected with FLAG-VP3 or empty vectors for 24 h, and samples were analyzed by Transmission electron microscopy (TEM) to show autophagosome. (D, E) HEK293T cells were transfected with the indicated plasmids, and cell lysates were immunoprecipitated with FLAG or GFP antibodies, followed by a western blot with GFP and FLAG antibodies. GAPDH was used as a sample loading control. (F) PK-15 cells were co-transfected with GFP-LC3B and FLAG-VP3 plasmid or empty vector for 24 h, and cells were then incubated with anti-FLAG (red), GFP (green), and DAPI (blue) for immunofluorescence staining and analyzed by confocal microscopy. (G, H) HEK293T cells were transfected with the indicated plasmids, and cell lysates were immunoprecipitated with FLAG or HA antibodies, followed by a western blot with HA and FLAG antibodies. GAPDH was used as a control to show the even loading of samples. (I) PK-15 cells were co-transfected with FLAG-VP3 and HA-SQSTM1 plasmid or empty vector for 24 h. Cells were then incubated with anti-FLAG (red), anti-HA (green), and DAPI (blue) for immunofluorescence staining and analyzed by confocal microscopy. (J) PK-15 cells were co-transfected with HA-HDAC8 and GFP-LC3B together with FLAG-VP3 plasmids or empty vector plasmid for 24 h, and cells were then incubated with anti-HA (red), GFP (green), and DAPI

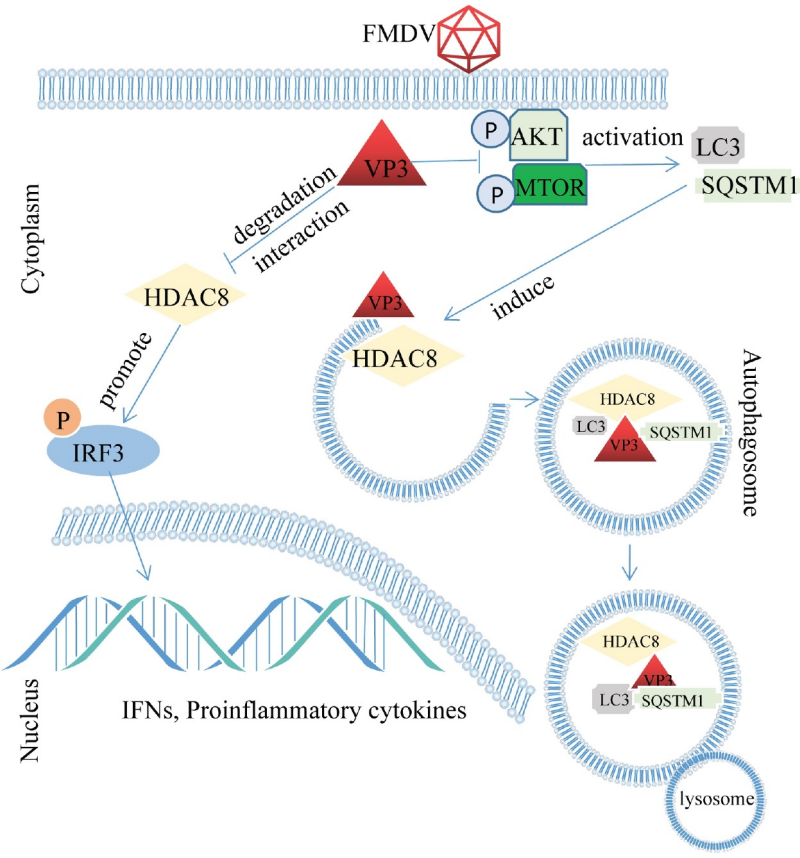

Figure 7. Schematic representation shows the model of FMDV structural protein VP3 interacts with and promotes HDAC8 autophagic degradation via the AKT-MTOR-ATG5 pathway. HDAC8 is involved in innate immune signaling pathways, the overexpression of HDAC8 increases the phosphorylation of TBK1 and IRF3, eventually promoting the expression of interferon-stimulated and proinflammatory cytokines genes. To counteract the antiviral function of HDAC8, FMDV structural protein VP3 induces autophagy by interacting with LC3 and SQSTM1 to degrade HDAC8. Furthermore, VP3 inhibits the phosphorylation of AKT and MTOR to promote HDAC8 autophagic degradation through the AKT-MTOR-ATG5 pathway to facilitate FMDV replication.

cargo receptor SQSTM1, thus inhibiting IFN production [64]. In our study, HDAC8 was shown to potentiate antiviral response. FMDV VP3 protein promoted the autophagic degradation of HDAC8, suggesting the involvement of autophagy in regulating immune responses. More investigations are needed to explore the regulation mechanism of HDAC8 during virus infection.

Protein acetylation has emerged as a key regulatory mechanism for autophagy. Many proteins functioning at different stages of the autophagy pathway have been identified as targets of acetylation [19,20,64–66]. ULK1, PIK3C3, and BECN1, key factors to promote phagophore formation and expansion, were acetylated by histone acetyltransferases KAT5/TIP60 and EP300/p300 [19,27,67]. LC3, which controls a key process in autophagy, was acetylated by EP300 or CREBBP at K49 and K51, which plays a negative role in autophagy by suppressing the redistribution of nuclear LC3 into the cytoplasm [68]. Autophagy-related genes *ATG5*, *ATG7*, and *ATG12* were also found acetylated by EP300 [69], while class III HDACs SIRT1 acted as major deacetylase that removed the acetyl group from the acetylated lysine of ATG5, ATG7 and LC3 [70]. Besides the above research, HDAC6 deacetylates CTTN (cortactin) and promotes autophagosome-lysosome fusion, eventually facilitating autophagy [66]. How acetylation regulates autophagic functions is still unclear, future studies need to explore more HATs and HDACs functioning in autophagy.

Furthermore, pathogenicity and lethality should be investigated *in vivo*. Singh *et al.* reported that females were subfertile when HDAC8 was knocked out prior to the pre-meiotic S phase and cohesion establishment (Vasa-Cre) [71]. Our study found that HDAC8 was degraded through the autophagy pathway during FMDV infection. Whether HDAC8 or other HDACs are involved in the regulation of autophagy deserves further investigation.

The VP3 protein of FMDV comprises 220 amino acid residues and is the most conserved of all the structural proteins of picornaviruses [72]. Previous studies have

(blue) for immunofluorescence staining and analyzed by confocal microscopy. (K) PK-15 cells were co-transfected with FLAG-VP3 plasmids and HA-HDAC8 plasmid for 24 h and maintained in the presence or absence of SC79 (5, 10, 20, 30 μM) respectively for 12 h. HA, HDAC8, AKT, p-AKT, MTOR, p-MTOR, LC3B, SQSTM1, and FLAG were analyzed by western blot. GAPDH was used as a control to show the even loading of samples. (L) Wild type and *ATG5*-KO PK-15 cells were seeded in 6-well plates, and the monolayer cells were co-transfected with 0, 1.0, 2.0 μg FLAG-VP3 (O strain) and 1.0 μg HA-HDAC8 expressing plasmids for 24 h. Expression of HA-HDAC8, endogenous HDAC8, SQSTM1, LC3B, ATG5, and FLAG was determined by western blot. GAPDH was used as a control to show the even loading of samples.

shown that FMDV VP3 inhibits the IFN signaling pathway by disrupting *MAVS/VISA* mRNA or degrading JAK1 [73]. Our study showed that VP3 promotes the autophagic degradation of HDAC8, it is plausible to speculate that some host factors may also be recruited and involved in the modification and degradation of HDAC8. Further studies could focus on identifying HDAC8 interaction proteins during virus infection. More importantly, despite being a member of the class I HDAC family, HDAC8 differs from other HDACs. The C-terminal (50–111 amino acids) protein binding domain of the other class I HDACs is absent in HDAC8 [74]. The size and composition of the N-terminal L1 loop of HDAC8 also differ from the other class I HDACs. It forms a large portion on one side of the active site and even leads to the expansion of the protein surface [75]. These unique characteristics of HDAC8 made it an attractive target for further investigation.

Materials and methods

Ethics statements

Studies with the Foot-and-Mouth Disease virus were conducted in a biosafety level 3 laboratory approved by Lanzhou Veterinary Research Institute, Chinese Academy of Agricultural Sciences.

Cells, viruses, and plasmids

Baby hamster kidney cells (BHK-21 cell), Human embryonic kidney 293T cells (293T cell), and porcine kidney cells (PK-15 cell) were purchased from ATCC (GNHa10, SCSP-502, BH-C706) and maintained in Dulbecco's modified Eagle's medium (DMEM; JSBio, 66001) supplemented with 10% fetal bovine serum (FBS; Aus GeneX, C0227) and 1% penicillin-streptomycin (Gibco/Thermo Scientific, 10378016) in a humidified incubator at 37°C with 5% CO_2. FMDV O/BY/2010 strain is stored in the National FMD Reference Laboratory (Lanzhou, Gansu, P.R. China). All virus-related experiments were conducted in the biosafety level-3 (BSL-3) Laboratory of Lanzhou Veterinary Research Institute, following the standard protocols and biosafety regulations provided by the Institutional Biosafety Committee. *HDAC8*-knockout (KO) cell lines were established using the CRISPR-Cas9 system following the published protocols [76]. Two pairs of the small guide RNAs (sgRNA) targeting the *HDAC8* gene of BHK-21 cells and PK-15 cells were designed using the CRISPR tool to establish the *HDAC8*-KO cell lines. Two sgRNAs were annealed and ligated to the pSpCas9 (BB) plasmid. The molecularly confirmed plasmids were transfected in BHK-21 cells and PK-15 cells, 3 μg puromycin was added per 1 ml of DMEM supplements, and the medium was renewed every 2 days. After puromycin selection, a single-cell clone was selected by the cloning ring anchoring method. The obtained monoclonal cell lines were identified by sequencing and western blot. *ATG5*-knockout (KO) in the PK-15 cell line was kindly gifted by Prof. Zhiyong Li (School of Basic Medical Sciences, Wenzhou Medical University).

pcDNA 3.1, GFP-LC3B, and HA-SQSTM1 plasmids were preserved in our lab. FLAG-VP0, FLAG-VP1, FLAG-VP2, FLAG-VP3, FLAG-2A2B, FLAG-2B, FLAG-2C, FLAG-3A, FLAG-3Cpro, and FLAG-3D were constructed and preserved in our Lab. HA-HDAC8, FLAG-VP3 (Asia 1 strain), FLAG-VP3 (A strain), FLAG-VP3 (1–168), FLAG-VP3 (169–315), FLAG-VP3 (316–465), and FLAG-VP3 (466–660) plasmids were obtained from Genecreate Company (Wuhan, China). *HDAC8* knockout plasmids were constructed by subcloning the sgRNA (BHK-21 sgRNA GGTTTCCCCGGCTTCCTAAA, PK-15 sgRNA AAACTCCGGATCCGGCTTTTT TCGC) into pSpCas9-puro plasmid from Addgene (48137, deposited by our lab) following the protocol provided by Dr. Feng Zhang's lab [76].

Western blot analyses and immunoprecipitations

Cell precipitate was lysed in RIPA Lysis Buffer (Thermo Fisher Scientific, 78501) containing a 1% protease inhibitor cocktail (Thermo Fisher Scientific, 87786). Total protein concentrations were quantified using the BCA Protein Assay kit obtained from Thermo scientific company. Equal amounts of protein samples were separated by sodium dodecyl sulfate-polyacrylamide gel electrophoresis (SDS-PAGE) and transferred to a polyvinylidene difluoride (PVDF) membrane. Then, the membrane was blocked with 5% skim milk at RT for 1 h, and the membranes were incubated with primary antibody overnight at 4°C. Western blot analyses were performed to detect the specific proteins with appropriate primary antibodies from different companies. Among them, HDAC8 (E7F5K), p-TBK1 (D52C2), TBK1 (E8I3G), p-IRF3 (E7J8G), IRF3 (D6I4C), p-AKT (D9E), AKT (11E7), p-MTOR (D9C2), MTOR (7C10), ATG5 (D5G3), and SQSTM1/p62 (D6M5X) were purchased from Cell Signaling Technology (Shanghai, China). LC3B (T55992), ACTB/β-actin (T40104), GAPDH (M20006), TUBB/tubulin (M20005), HA (M10004), FLAG (M20008), and GFP (7G9) were purchased from Abmart (Shanghai, China). VP3 antibody was preserved in our lab. MG132, CQ, 3-MA, SC79, and Baf-A_1 were purchased from MedChemExpress (HY-13259, HY-17589A, HY-19312, HY-18749 and HY-100558). SAHA, TSA, MGCD0103, NIC, and PCI34051 were preserved in our Lab. FMDV (VP0, VP3, VP1) polyclonal antibody was kindly gifted by Prof. Huichen Guo (Lanzhou Veterinary Research Institute, Chinese Academy of Agricultural Science). After that, the membrane was washed with TBS-T buffer three times before incubation with HRP-conjugated secondary antibody (Thermo Fisher Scientific, Goat anti-Rabbit 31,460, Goat anti-Mouse 31,430) for 1 h, followed by chemiluminescent detection.

Co-immunoprecipitation assay

HEK-293T cells were cultured in 60-mm dishes, and the monolayer cells were co-transfected with the indicated plasmids. The transfected cells were washed with PBS (Solarbio LIFE SCIENCES, P1032) and lysed with 600 μl of lysis buffer (Thermo Fisher Scientific, 87788). Anti-FLAG, anti-GFP, or anti-HA antibodies (Abmart, M20008, M20004, M20003) were used to immunoprecipitate the interacted proteins by 50% (v:v) slurry of GammaBind G Plus-Sepharose (Abmart,

Table 1. The primers used for quantitative real-time PCR.

Primer	Sequence (5′→3′)
VP1-F	GACAACACCACCAACCCA
VP1-R	CCTTCTGAGCCAGCACTT
GAPDH-F	ACATGGCCTCCAAGGAGTAAGA
GAPDH-R	GATCGAGTTGGGGCTGTGACT
Ma-HDAC8-F	GGTTTCCCCGGCTTCCTAAA
Ma-HDAC8-R	ACATCTCCCAGCATGCTCTG
SUS-HDAC8-F	CAGTGCATATGCCTCAATCA
SUS-HDAC8-R	TGATTGAGGCATATGCACTG
SUS-TNF-F	CGTTGTAGCCAATGTCAAAGCC
SUS-TNF-R	TGCCCAGATTCAGCAAAGTCCA
SUS-IFIT2-F	CTGGCAAAGAGCCCTAAGGA
SUS-IFIT2-R	CTCAGAGGGTCAATGGAATTCC
SUS-OAS-F	AAGCATCAGAAGCTTTGCATCTT
SUS-OAS-R	CAGGCCTGGGTTTCTTGAGTT
SUS-IFNB-F	GCTAACAAGTGCATCCTCCAAA
SUS-IFNB-R	AGCACATCATAGCTCATGGAAAGA
SUS-CCL5-F	TACAGCTACCATGAAGGTCTCCAC
SUS-CCL5-R	TGATGCTGGAGCGCAGAG

A10001) overnight at 4°C. The precipitates were subjected to western blot.

Virus infection, RNA extraction, and RT-Qpcr

BHK-21 cells and PK-15 cells were cultured in 60-mm dishes to reach an approximate 90% confluence, which was washed once with PBS and incubated with FMDV at a multiplicity of infection (MOI) of 0.1 at 37°C for 1 h. Then, the cells were washed with PBS and cultured in 3 mL of FBS-free DMEM. After infection, the supernatant was removed, and 1 mL of TRIzol Reagent (Invitrogen, 15596026CN) was added to each dish. Total RNA was isolated according to the manufacturer's instructions. RNA (1 μg) was used as the template for cDNA synthesis using PrimeScript^{TM} RT reagent Kit with gDNA Eraser (TAKARA, 639549). cDNA was then subjected to real-team PCR quantification using SYBR green Premix Ex Taq II (TAKARA, RR650A). The GAPDH gene was used as an internal control. The primers used in the experiment are listed in Table 1. All the experiments were repeated at least three times, and relative mRNA expression levels were calculated using the threshold cycle ($2^{-\Delta\Delta Ct}$) method.

The growth characteristics of FMDV in NC (negative control) and *HDAC8*-KO cells were detected by qRT-PCR. *HDAC8*-KO cells and NC cells were seeded in 6-well plates (1×10^6 cells/well) for 24 h and then infected with the FMDV at an MOI of 0. 1 when confluence reached 90%. All the experiments were repeated at least three times.

$TCID_{50}$ assay

Viral titrations were determined using $TCID_{50}$ assay. BHK-21 cells were seeded in 96-well plates with 90% confluence, and a series of 10-fold serial dilutions from 10^{-1} to 10^{-8} of virus samples were prepared in another plate. One hundred microliters of the above samples were added to each well, and the plates were incubated at 37°C for 1 h. Then, the inoculum was removed, and cells were cultured in DMEM supplemented with 1% FBS for 72 h. All plates were analyzed by microscopic examination to determine the cytopathogenic effect (CPE). $TCID_{50}$ was calculated by the Reed-Muench method [77].

Indirect immunofluorescence microscopy

The cells were seeded in NuncTM glass bottom dishes (NEST, GBD-35-20) and cultured to a confluence of approximately 60–70%, then fixed with an acetone/methanol mixture (1:1) for 10 min at −20°C. Normal goat serum (5%; Life Technologies, 16210064) in PBS was used as the blocking buffer, and the fixed cells were washed with PBS and blocked for 1 h at 37°C. The anti-FLAG and anti-HA primary antibodies were subsequently incubated overnight at 4°C. Cells were washed with PBS five times at room temperature (RT; 10 min each time). The fluorochrome-conjugated secondary antibodies (Alexa Fluor® 488 and 546, 1:1000; Thermo Fisher Scientific, A11070 and A11018) were incubated with the cells in the dark for 1 h and washed with Tris-buffered saline (Na_2HPO_4, KH_2PO_4, NaCl, KCl, liquid, sterile-filtered, pH 7.6) three times at RT (10 min each time). The cells were incubated with 4', 6-diamidino-2-phenylindole (DAPI; Roche, Diagnostics, 10236276001) for 10 min at RT to stain the nuclei. The stained cells and fluorescence were visualized using a Nikon Eclipse 80i fluorescence microscope with appropriate settings. The microscopy images were processed using NIS Elements F 2.30 software.

Electron microscopy

Electron microscopy was performed as described [78]. Briefly, cell samples were washed three times with 1×PBS, trypsinized, and collected by centrifugation at 1000×g for 5 min. The cell pellets were fixed in 2.5% glutaraldehyde (Sigma-Aldrich, G6257), 2% paraformaldehyde in 0.1 M cacodylate (pH 7.2) buffer for 2 h at room temperature, washed in cacodylate, post-fixed with 2% osmium tetroxide (OsO_4; Electron Microscopy Sciences, 19150) supplemented with 1.5% potassium ferrocyanide (45 min, 4°C), washed in water, dehydrated with sequential washes in a graded series of ethanol (Sinopharm Chemical Reagent, 10009218), and embedded in Epon (Sigma-Aldrich, 45345). Ultrathin sections of cell monolayers were prepared with a Reichert UltracutS ultramicrotome (Leica Microsystems, Germany) and contrasted with uranyl acetate and lead citrate. Images of thin sections were observed under a transmission electron microscope (Hitachi, HT7700, Japan).

Statistical analysis

This study's quantified results were presented as mean values ±s.e of three independent experiments. The student's t-test was used to determine statistical significance. $^{*}p < 0.05$was considered significant, and $^{**}p < 0.01$was highly significant.

Acknowledgements

We thank Prof. Huichen Guo, Lanzhou Veterinary Research Institute, Chinese Academy of Agricultural Science, for providing the FMDV (VP0, VP3, VP1) antibody. We thank the staff at the Instrument Center, Lanzhou Veterinary Research Institute, and Chinese Academy of Agricultural Science for advice and assistance in Confocal laser scanning microscopy sample observation and data collection.

Disclosure statement

No potential conflict of interest was reported by the authors.

Funding

This research was financially supported by the Agricultural Science and Technology Innovation Program of CAAS (CAAS-ASTIP-2021-LVRI), National Key R&D Program of China (2021YFD1800300) the Key Development and Research Foundation of Gansu (21YF5WA153), and the Natural Science Foundation Project of China (Grant no. 32202779).

References

[1] Mizushima N, Levine B. Autophagy in mammalian development and differentiation. Nat Cell Biol. 2010;12(9):823–830. doi: 10.1038/ncb0910-823

[2] Mizushima N, Yoshimori T, Ohsumi Y. The role of Atg proteins in autophagosome formation. Annu Rev Cell Dev Biol. 2011;27(1):107–132. doi: 10.1146/annurev-cellbio-092910-154005

[3] Viret C, Duclaux-Loras R, Nancey S, et al. Selective autophagy receptors in antiviral defense. Trends Microbiol. 2021;29(9):798–810. doi: 10.1016/j.tim.2021.02.006

[4] Kumar S, Jain A, Farzam F, et al. Mechanism of Stx17 recruitment to autophagosomes via IRGM and mammalian Atg8 proteins. J Cell Bio. 2018;217(3):997–1013. doi: 10.1083/jcb.201708039

[5] Gomez-Virgilio L, Silva-Lucero MD, Flores-Morelos DS, et al. Autophagy: a key regulator of homeostasis and disease: an overview of molecular mechanisms and modulators. Cells. 2022;11(15):2262. doi: 10.3390/cells11152262

[6] Mayer F, Heath R, Underwood E, et al. ADP regulates SNF1, the Saccharomyces cerevisiae homolog of AMP-activated protein kinase. Cell Metab. 2011;14(5):707–714. doi: 10.1016/j.cmet.2011.09.009

[7] Garcia D, Shaw R. AMPK: mechanisms of cellular energy sensing and restoration of metabolic balance. Molecular Cell. 2017;66(6):789–800. doi: 10.1016/j.molcel.2017.05.032

[8] Jiang H, Kan X, Ding C, et al. The multi-faceted role of autophagy during animal virus infection. Front Cell Infect Microbiol. 2022;12:858953. doi: 10.3389/fcimb.2022.858953

[9] Mizushima N, Komatsu M. Autophagy: renovation of cells and tissues. Cell. 2011;147(4):728–741. doi: 10.1016/j.cell.2011.10.026

[10] Mizushima N, Noda T, Yoshimori T, et al. A protein conjugation system essential for autophagy. Nature. 1998;395(6700):395–398. doi: 10.1038/26506

[11] Shelly S, Lukinova N, Bambina S, et al. Autophagy is an essential component of Drosophila immunity against vesicular stomatitis virus. Immunity. 2009;30(4):588–598. doi: 10.1016/j.immuni.2009.02.009

[12] Orvedahl A, MacPherson S, Sumpter R Jr., et al. Autophagy protects against Sindbis virus infection of the central nervous system. Cell Host Microbe. 2010;7(2):115–127. doi: 10.1016/j.chom.2010.01.007

[13] Viret C, Rozieres A, Faure M. Autophagy during early virus-host cell interactions. J Mol Biol. 2018;430(12):1696–1713. doi: 10.1016/j.jmb.2018.04.018

[14] Montespan C, Marvin SA, Austin S, et al. Multi-layered control of Galectin-8 mediated autophagy during adenovirus cell entry through a conserved PPxY motif in the viral capsid. PLOS Pathog. 2017;13(2):e1006217. doi: 10.1371/journal.ppat.1006217

[15] Grubman MJ, Baxt B. Foot-and-mouth disease. Clin Microbiol Rev. 2004;17(2):465–493. doi: 10.1128/CMR.17.2.465-493.2004

[16] Nayak A, Goodfellow IG, Belsham GJ. Factors required for the Uridylylation of the foot-and-mouth disease virus 3B1, 3B2, and 3B3 peptides by the RNA-dependent RNA polymerase (3Dpol) *in vitro*. J Virol. 2005;79(12):7698–7706. doi: 10.1128/JVI.79.12.7698-7706.2005

[17] O'Donnell V, Pacheco JM, LaRocco M, et al. Foot-and-mouth disease virus utilizes an autophagic pathway during viral replication. Virology. 2011;410(1):142–150. doi: 10.1016/j.virol.2010.10.042

[18] Gladue DP, O'Donnell V, Baker-Branstetter R, et al. Foot-and-mouth disease virus nonstructural protein 2C interacts with Beclin1, modulating virus replication. J Virol. 2012;86(22):12080–12090. doi: 10.1128/JVI.01610-12

[19] Berryman S, Brooks E, Burman A, et al. Foot-and-mouth disease virus induces autophagosomes during cell entry via a class III phosphatidylinositol 3-kinase-independent pathway. J Virol. 2012;86(23):12940–12953. doi: 10.1128/JVI.00846-12

[20] Sun P, Zhang S, Qin X, et al. Foot-and-mouth disease virus capsid protein VP2 activates the cellular EIF2S1-ATF4 pathway and induces autophagy via HSPB1. Autophagy. 2018;14(2):336–346. doi: 10.1080/15548627.2017.1405187

[21] Yang W, Li D, Ru Y, et al. Foot-and-mouth disease virus 3A protein causes upregulation of autophagy-related protein LRRC25 to inhibit the G3BP1-mediated RIG-Like helicase-signaling pathway. J Virol. 2020;94(8):e02086–19. doi: 10.1128/JVI.02086-19

[22] Ranjitha HB, Ammanathan V, Guleria N, et al. Foot-and-mouth disease virus induces PERK-mediated autophagy to suppress the antiviral interferon response. J Cell Sci. 2020;134(5):jcs240622. doi: 10.1242/jcs.240622

[23] Zhang R, Qin X, Yang Y, et al. STING1 is essential for an RNA-virus triggered autophagy. Autophagy. 2022;18(4):816–828. doi: 10.1080/15548627.2021.1959086

[24] Rodriguez Pulido M, Saiz M. Molecular mechanisms of foot-and-mouth disease virus targeting the host antiviral response. Front Cell Infect Microbiol. 2017;7:252. doi: 10.3389/fcimb.2017.00252

[25] Medina GN, Segundo FD, Stenfeldt C, et al. The different tactics of foot-and-mouth disease virus to evade innate immunity. Front Microbiol. 2018;9:2644. doi: 10.3389/fmicb.2018.02644

[26] Han S, Mao L, Liao Y, et al. Sec62 suppresses foot-and-mouth disease virus proliferation by promotion of IRE1α-RIG-I antiviral signaling. J Immunol (Baltimore, Md : 1950). 2019;203(2):429–440. doi: 10.4049/jimmunol.1801546

[27] Fan X, Han S, Yan D, et al. Foot-and-mouth disease virus infection suppresses autophagy and NF-small ka, CyrillicB antiviral responses via degradation of ATG5-ATG12 by 3C(pro). Cell Death Dis. 2017;8(1):e2561. doi: 10.1038/cddis.2016.489

[28] Wu J, Zhang Z, Teng Z, et al. Sec62 regulates endoplasmic reticulum stress and autophagy balance to affect foot-and-mouth disease virus replication. Front Cell Infect Microbiol. 2021;11:707107. doi: 10.3389/fcimb.2021.707107

[29] Hildmann C, Riester D, Schwienhorst A. Histone deacetylases–an important class of cellular regulators with a variety of functions. Appl Microbiol Biotechnol. 2007;75(3):487–497. doi: 10.1007/s00253-007-0911-2

[30] Li G, Tian Y, Zhu W. The roles of histone deacetylases and their inhibitors in cancer therapy. Front Cell Dev Biol. 2020;8:576946. doi: 10.3389/fcell.2020.576946

[31] Seto E, Yoshida M. Erasers of histone acetylation: the histone deacetylase enzymes. Cold Spring Harb Perspect Biol. 2014;6(4):a018713. doi: 10.1101/cshperspect.a018713

[32] Grabiec A, Potempa J. Epigenetic regulation in bacterial infections: targeting histone deacetylases. Crit Rev Microbiol. 2018;44(3):336–350. doi: 10.1080/1040841X.2017.1373063

[33] Minucci S, Pelicci PG. Histone deacetylase inhibitors and the promise of epigenetic (and more) treatments for cancer. Nat Rev Cancer. 2006;6(1):38–51. doi: 10.1038/nrc1779

[34] Yang XJ, Seto E. The Rpd3/Hda1 family of lysine deacetylases: from bacteria and yeast to mice and men. Nat Rev Mol Cell Biol. 2008;9(3):206–218. doi: 10.1038/nrm2346

[35] Falkenberg KJ, Johnstone RW. Histone deacetylases and their inhibitors in cancer, neurological diseases and immune disorders. Nat Rev Drug Discov. 2014;13(9):673–691. doi: 10.1038/nrd4360

[36] Narita T, Weinert B, Choudhary C. Functions and mechanisms of non-histone protein acetylation. Nat Rev Mol Cell Biol. 2019;20(3):156–174. doi: 10.1038/s41580-018-0081-3

[37] Wang Q, Zhang Y, Yang C, et al. Acetylation of metabolic enzymes coordinates carbon source utilization and metabolic flux. Science. 2010;327(5968):1004–1007. doi: 10.1126/science.1179687

[38] Wilting RH, Yanover E, Heideman MR, et al. Overlapping functions of Hdac1 and Hdac2 in cell cycle regulation and haematopoiesis. Embo J. 2010;29(15):2586–2597. doi: 10.1038/emboj.2010.136
[39] Rahmani G, Sameri S, Abbasi N, et al. The clinical significance of histone deacetylase-8 in human breast cancer. Pathol Res Pract. 2021;220:153396. doi: 10.1016/j.prp.2021.153396
[40] Rroji O, Kumar A, Karuppagounder SS, et al. Epigenetic regulators of neuronal ferroptosis identify novel therapeutics for neurological diseases: HDACs, transglutaminases, and HIF prolyl hydroxylases. Neurobiology Of Disease. 2021;147:105145. doi: 10.1016/j.nbd.2020.105145
[41] Tang J, Yang Q, Xu C, et al. Histone deacetylase 3 promotes innate antiviral immunity through deacetylation of TBK1. Protein Cell. 2021;12(4):261–278. doi: 10.1007/s13238-020-00751-5
[42] Yang Q, Tang J, Pei R, et al. Host HDAC4 regulates the antiviral response by inhibiting the phosphorylation of IRF3. J Mol Cell Biol. 2019;11(2):158–169. doi: 10.1093/jmcb/mjy035
[43] Haberland M, Montgomery RL, Olson EN. The many roles of histone deacetylases in development and physiology: implications for disease and therapy. Nat Rev Genet. 2009;10(1):32–42. doi: 10.1038/nrg2485
[44] Oh J, Broyles SS. Host cell nuclear proteins are recruited to cytoplasmic vaccinia virus replication complexes. J Virol. 2005;79 (20):12852–12860. doi: 10.1128/JVI.79.20.12852-12860.2005
[45] Nusinzon I, Horvath CM. Positive and negative regulation of the innate antiviral response and beta interferon gene expression by deacetylation. Mol Cell Biol. 2006;26(8):3106–3113. doi: 10.1128/MCB.26.8.3106-3113.2006
[46] Meng J, Liu X, Zhang P, et al. Rb selectively inhibits innate IFN-beta production by enhancing deacetylation of IFN-beta promoter through HDAC1 and HDAC8. J Autoimmun. 2016;73:42–53. doi: 10.1016/j.jaut.2016.05.012
[47] Yamauchi Y, Boukari H, Banerjee I, et al. Histone deacetylase 8 is required for centrosome cohesion and influenza a virus entry. PLOS Pathog. 2011;7(10):e1002316. doi: 10.1371/journal.ppat.1002316
[48] Xia B, Lu J, Wang R, et al. MiR-21-3p regulates influenza a virus replication by targeting histone deacetylase-8. Front Cell Infect Microbiol. 2018;8:175. doi: 10.3389/fcimb.2018.00175
[49] Finnin M, Donigian J, Cohen A, et al. Structures of a histone deacetylase homologue bound to the TSA and SAHA inhibitors. Nature. 1999;401(6749):188–193. doi: 10.1038/43710
[50] Duvic M, Talpur R, Ni X, et al. Phase 2 trial of oral vorinostat (suberoylanilide hydroxamic acid, SAHA) for refractory cutaneous T-cell lymphoma (CTCL). Blood. 2007;109(1):31–39. doi: 10.1182/blood-2006-06-025999
[51] Zhou N, Moradei O, Raeppel S, et al. Discovery of N-(2-aminophenyl)-4-[(4-pyridin-3-ylpyrimidin-2-ylamino) methyl]benzamide (MGCD0103), an orally active histone deacetylase inhibitor. J Med Chem. 2008;51(14):4072–4075. doi: 10.1021/jm800251w
[52] Taori K, Paul V, Luesch H. Structure and activity of largazole, a potent antiproliferative agent from the Floridian marine cyanobacterium Symploca sp. J Am Chem Soc. 2008;130(6):1806–1807. doi: 10.1021/ja7110064
[53] Ekanayaka P, Shin S, Weeratunga P, et al. Foot-and-mouth disease virus 3C protease antagonizes interferon signaling and C142T substitution attenuates the FMD virus. Front Microbiol. 2021;12:737031. doi: 10.3389/fmicb.2021.737031
[54] Yi J, Peng J, Ren J, et al. Degradation of host proteins and apoptosis induced by foot-and-mouth disease virus 3C protease. Pathogens. 2021;10(12):1566. doi: 10.3390/pathogens10121566
[55] Park JY, Juhnn YS. cAMP signaling increases histone deacetylase 8 expression by inhibiting JNK-dependent degradation via autophagy and the proteasome system in H1299 lung cancer cells. Biochem Biophys Res Commun. 2016;470(2):336–342. doi: 10.1016/j.bbrc.2016.01.049
[56] Nakatogawa H, Ichimura Y, Ohsumi Y. Atg8, a ubiquitin-like protein required for autophagosome formation, mediates membrane tethering and hemifusion. Cell. 2007;130(1):165–178. doi: 10.1016/j.cell.2007.05.021
[57] Buchkovich N, Yu Y, Zampieri C, et al. The TORrid affairs of viruses: effects of mammalian DNA viruses on the PI3K-Akt-Mtor signalling pathway. Nat Rev Microbiol. 2008;6(4):266–275. doi: 10.1038/nrmicro1855
[58] Mizushima N, Yoshimori T, Levine B. Methods in mammalian autophagy research. Cell. 2010;140(3):313–326. doi: 10.1016/j.cell.2010.01.028
[59] Takeuchi O, Akira S. Pattern recognition receptors and inflammation. Cell. 2010;140(6):805–820. doi: 10.1016/j.cell.2010.01.022
[60] Schlee M, Hartmann G. Discriminating self from non-self in nucleic acid sensing. Nat Rev Immunol. 2016;16(9):566–580. doi: 10.1038/nri.2016.78
[61] Liu Y, Zhou T, Hu J, et al. Targeting selective autophagy as a therapeutic strategy for viral infectious diseases. Front Microbiol. 2022;13:889835. doi: 10.3389/fmicb.2022.889835
[62] Wang Z, Chen J, Wu X, et al. PCV2 targets cGAS to inhibit type I interferon induction to promote other DNA virus infection. PLOS Pathog. 2021;17(9):e1009940. doi: 10.1371/journal.ppat.1009940
[63] Zeng Y, Xu S, Wei Y, et al. The PB1 protein of influenza a virus inhibits the innate immune response by targeting MAVS for NBR1-mediated selective autophagic degradation. PLOS Pathog. 2021;17(2):e1009300. doi: 10.1371/journal.ppat.1009300
[64] Sui C, Xiao T, Zhang S, et al. SARS-CoV-2 NSP13 inhibits type I IFN production by degradation of TBK1 via p62-dependent selective autophagy. J Immunol. 2022;208(3):753–761. doi: 10.4049/jimmunol.2100684
[65] Shen Q, Shi Y, Liu J, et al. Acetylation of STX17 (syntaxin 17) controls autophagosome maturation. Autophagy. 2021;17 (5):1157–1169. doi: 10.1080/15548627.2020.1752471
[66] You Z, Jiang WX, Qin LY, et al. Requirement for p62 acetylation in the aggregation of ubiquitylated proteins under nutrient stress. Nat Commun. 2019;10(1):5792. doi: 10.1038/s41467-019-13718-w
[67] Sun T, Li X, Zhang P, et al. Acetylation of Beclin 1 inhibits autophagosome maturation and promotes tumour growth. Nat Commun. 2015;6(1):7215. doi: 10.1038/ncomms8215
[68] Huang R, Xu Y, Wan W, et al. Deacetylation of nuclear LC3 drives autophagy initiation under starvation. Mol Cell. 2015;57 (3):456–466. doi: 10.1016/j.molcel.2014.12.013
[69] Lee IH, Finkel T. Regulation of autophagy by the p300 acetyltransferase. J Biol Chem. 2009;284(10):6322–6328. doi: 10.1074/jbc.M807135200
[70] Lee IH, Cao L, Mostoslavsky R, et al. A role for the NAD-dependent deacetylase Sirt1 in the regulation of autophagy. Proc Natl Acad Sci USA. 2008;105(9):3374–3379. doi: 10.1073/pnas.0712145105
[71] Singh V, Yueh W, Gerton J, et al. Oocyte-specific deletion of Hdac8 in mice reveals stage-specific effects on fertility. Reproduction. 2019;157(3):305–316. doi: 10.1530/REP-18-0560
[72] Mason P, Grubman M, Baxt B. Molecular basis of pathogenesis of FMDV. Virus Res. 2003;91(1):9–32. doi: 10.1016/S0168-1702(02)00257-5
[73] Li D, Wei J, Yang F, et al. Foot-and-mouth disease virus structural protein VP3 degrades Janus kinase 1 to inhibit IFN-gamma signal transduction pathways. Cell Cycle. 2016;15(6):850–860. doi: 10.1080/15384101.2016.1151584
[74] Somoza JR, Skene RJ, Katz BA, et al. Structural snapshots of human HDAC8 provide insights into the class I histone deacetylases. Structure. 2004;12(7):1325–1334. doi: 10.1016/j.str.2004.04.012
[75] Chakrabarti A, Oehme I, Witt O, et al. HDAC8: a multifaceted target for therapeutic interventions. Trends Pharmacol Sci. 2015;36(7):481–492. doi: 10.1016/j.tips.2015.04.013
[76] Ran F, Hsu P, Wright J, et al. Genome engineering using the CRISPR-Cas9 system. Nat Protoc. 2013;8(11):2281–2308. doi: 10.1038/nprot.2013.143
[77] Reed L, Muench H. A simple method of estimating fifty er cent endpoints. Am J Epidemiol. 1938;27:493–497. doi: 10.1093/oxfordjournals.aje.a118408
[78] Li M, Jiang X, Liu D, et al. Autophagy protects LNCaP cells under androgen deprivation conditions. Autophagy. 2008;4(1):54–60. doi: 10.4161/auto.5209